XX (335149 1)

The Creswellian (Pleistocene) human upper limb remains from Gough's Cave (Somerset, England)

STEVEN E. CHURCHILL

Department of Biological Anthropology and Anatomy, Duke University, Durham, NC 27708, USA

SYNOPSIS. The human remains from the Pleistocene deposits in Gough's Cave include more than 25 fragmentary elements from the pectoral girdle and upper limb. These remains are described here, and represent at least three and most likely four individuals (two larger, possibly male individuals and two smaller, possibly female or juvenile individuals). Many of these fragmentary bones show marks made by stone tools, including one element (a right radius) with engraving, suggesting human damage before they were deposited.

INTRODUCTION

The human upper limb remains from the Creswellian levels of Gough's Cave, like those of the lower limb (Trinkaus, this volume), are highly fragmentary. In some cases multiple pieces have been refitted along peri-/post-mortem breaks (the conjoined pieces now being cataloged as a single element), but the assemblage overall remains a fragmentary one, with little possibility of associating pieces by individual. Evidence of human modification of the skeletal elements is abundant (see Cook, 1986; Currant *et al.*, 1989; Andrews & Fernandez-Jalvo, this series of papers), and humans were undoubtedly at least partly responsible for the damage that is characteristic of this assemblage.

The following description provides inventory information (using the current Natural History Museum catalogue numbers [M.54XXX series], followed by an excavation number or numbers), along with observations on the state or preservation and the morphology of each element. Osteometric comparisons were made, where possible, with comparably-aged (*i.e.*, terminal Pleistocene) European fossil humans. The comparative sample derives primarily from Magdalenian/Epigravettian contexts (*ca.* 16 – 10 kya), and includes male specimens Arene Candide 2, 4, 5, 10 and 12, Chancelade 1, Gough's Cave 1, Le Placard 16, Neuessing 2, Oberkassel 1, Rocheriel 1, Romanelli 1, Romito 3, and Veyrier 1, 7 and 9 (Paoli *et al.*, 1980; Vallois, 1941–46; Seligman & Parsons, 1914; Breuil, 1912; Gieseler, 1977; Verworn *et al.*, 1919; Boule & Vallois, 1946; Stasi & Regalia, 1904; Pittard & Sauter, 1945), and female specimens Arene Candide 13 and 14, Bruniquel 24, Cap Blanc 1, Farincourt 1, Oberkassel 2, Romito 4 and St. Germain-la-Rivière 4 (Paoli *et al.*, 1980; Genet-Varcin & Miquel, 1967; Bonin, 1935; Sauter, 1957; Verworn *et al.*, 1919). All comparative data were collected by the author on original specimens.

Five specimens – three claviculae, one humerus and one ulna – had diaphyses reasonably complete to estimate cross-sectional geometric properties. The small number of specimens of each element and a general lack of comparative data combine to limit the conclusions that can be drawn from structural analysis of diaphyseal morphology. The cross-sectional data are thus included merely as a supplement to the morphological descriptions.

Diaphyseal cross-sections were reconstructed from radiographs and external contour moulds for the midshaft (claviculae and humeri) or mid-proximal (ulnae) diaphyses. Subperiosteal contour moulds were taken perpendicular to the diaphyseal axis, using dental putty moulds (Cuttersil Putty Plus: Heraeus Kulzer Inc.), at 50% (midshaft) or 65% (mid-proximal) of biomechanical length (measured from the distal end). The moulds where photostatically reproduced on paper to provide the subperiosteal (outside) contour of the cross-section. In the case of claviculae, ventral, dorsal, superior and inferior cortical thickness dimensions were measured from superoinferior and dorsoventral radiographs. For humeri and ulnae, anterior, posterior, medial and lateral cortical thickness dimensions were measured from mediolateral and anteroposterior radiographs. Subperiosteal dimensions from the original specimens were compared with those from the radiographs to determine the degree of parallax distortion and thus allow for algebraic correction of cortical thickness measurements. The cortical dimensions were used along with the subperiosteal contour to interpolate the endosteal contour. The resultant cross-sections were manually digitized and geometric properties were computed using a PC-DOS version (Eschman, 1990) of SLICE (Nagurka & Hayes, 1980).

SLICE calculates the total subperiosteal (TA) and cortical (CA) areas, second moments of area about the superoinferior (clavicle) or anteroposterior (humerus and ulna) (I_x) and dorsoventral (clavicle) or mediolateral (humerus and ulna) (I_y) axes, and the maximum (I_{max}) and minimum (I_{min}) second moments of area. Geometric analysis of cross-sections provides measures of the contribution of bone geometry to the resistance of biomechanical loads: in the case of cortical area, to axial compressive and tensile loads; for second moments of area, to bending loads. Medullary area (MA) can be determined from total and cortical areas (MA = TA – CA). The polar moment of area (J, or I_p) is a measure of torsional rigidity and overall strength, and can be determined as the sum of any two perpendicular second moments of area ($J = [I_x + I_y] = [I_{max} + I_{min}]$).

In addition to the measures of bone rigidity outlined above, three cross-sectional shape indices were computed to better illustrate the morphology of the Gough's Cave Creswellian upper limb material. The first of these is percent cortical area (%CA = 100*CA/TA), which serves as a simple measure of the degree of cortical occlusion of the medullary space. Ratios of second moments of area provide information about diaphyseal shape (at the location of the cross section) with respect to anatomical axes (I_x/I_y) or with respect to the axis of maximum bending rigidity (I_{max}/I_{min}).

CLAVICULAR REMAINS

M.54053 (M23.1/1) (Fig. 1)
Left
This is a complete clavicle. With the exception of some abrasion and erosion of the sternal end on the inferior margin and to a portion of the superior edge, and some very slight damage to the lateral edge of the acromial articular surface, the bone is in a perfect state of preservation. There is marked curvature to both the medial and lateral ends of the shaft. There is very little torsion to the shaft, except at the very proximal end, such that the long axis of the sternal articulation is oriented at 135° to the horizontal plane of the acromial end. Medially the shaft cross-section forms an isosceles triangle with the base superior, while laterally the shaft is more rectangular in section, with the superoinferior dimension being the smaller.

Fig. 1   Left clavicle, M.54053, natural size. **1A,** superior; **1B,** inferior.
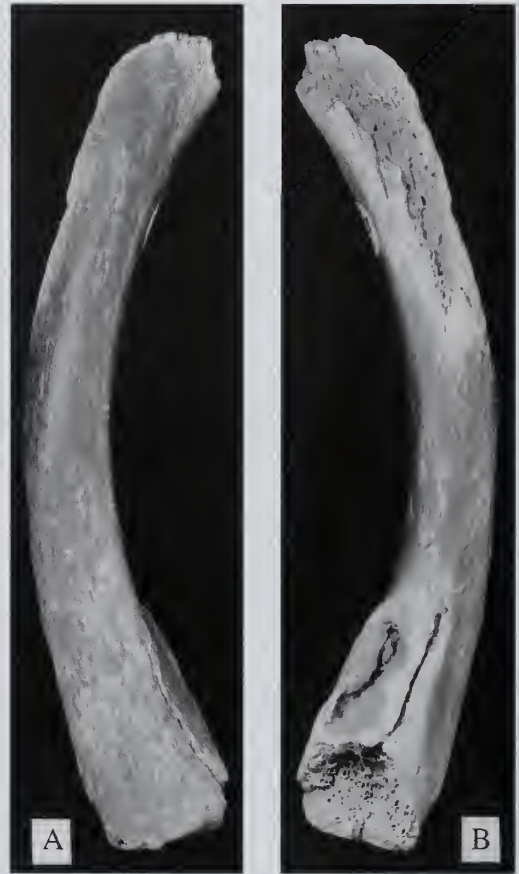

Fig. 2   Right proximal clavicle, M.54054, natural size. **2A,** superior; **2B,** inferior.

Cutmarks are evident on the medial inferior surface (around the costoclavicular ligament attachment area), near midshaft, and on the anterosuperior margin of the acromial facet (see Andrews & Fernandez-Jalvo, this series of papers).

Along the superior surface, there is very mild rugosity at the insertion area for *M. Sternocleidomastoideus*. There is a weak but clear crest delimiting the superior edge of the *M. pectoralis major* origin on the superoventral margin of the medial third of the shaft. Just lateral of midshaft this crest blends with the origination scar for *M. deltoideus*. Medially the *M. deltoideus* scar is rugose and well defined, laterally the muscle origin is marked by a clear crest superiorly and a rugose tubercle laterally, but the bone surface over most of this part of the origin area is not especially rugose. The insertion area for *M. trapezius* is marked by some smooth tubercles medially (just medial of the level of the conoid tubercle) and some rugosity just mediodorsal of the acromial articular surface. The superior surface of the acromial end is relatively smooth.

On the inferior surface, the origin of *M. sternohyoid* can be seen as a small patch of very slight rugosity. The costoclavicular ligament attachment is marked by a pit with small exostotic projections lining the dorsal edge of the ligament scar. The oval costoclavicular ligament scar is continued laterally as a rugose broad ridge extending roughly 29mm along the inferior shaft. This ridge may mark the inferior edge of *M. pectoralis major*, perhaps including some of the attachment area of *M. subclavius* and the clavipectoral fascia near midshaft. The conoid tubercle is well defined and large, and projects

dorsally and inferiorly. The trapezoid line is rugose and well defined. The dorsolateral surface of the acromial end has a number of rugose tubercles, perhaps indicating the attachment of *M. trapezius*.

There are no signs of degenerative changes on the sternal articular surface, while the acromial facet is pitted and vascular, with some very incipient lipping along the inferior border.

M.54054 (GC 89 022) (Fig. 2)
Right
This 108.7mm long fragment represents the proximal end of a right clavicle, preserving the superior portion of the sternal articular surface, most of the corpus laterally to the point of maximum curvature of the proximal shaft, and the superior and dorsal surfaces of the shaft to the proximal part of the *M. deltoideus* origination area (medial of the conoid tubercle). The inferior portion of the sternal end is broken away. In size and shape (including proximal shaft curvature) this specimen matches M.54053, with the exception that in M.54054 the sternal epiphyseal plate is unfused and missing. Oblique cutmarks are evident on the superior surface near the sternal end.

The *M. pectoralis major* appears to have been well developed in this individual. The superior line of attachment of the muscle begins as a projecting but only mildly rugose ridge on the anterosuperior margin of the clavicle just lateral of the sternal articular surface. The muscle attachment area is moderately rugose, and leaves a flattened surface laterally on the anterosuperior shaft that is almost continuous with the medial *M. deltoideus* attachment scar. Only a small portion of the *M. deltoideus* scar is preserved. Inferiorly, the costoclavicular ligament attachment area is a large, very deep and very rugose pit (Fig. 2B). A very clear ridge extends laterally from the costoclavicular ligament pit, marking the inferior extent of the *M. pectoralis major* muscle. There also appears to be a crest for *M. subclavius* extending from this ridge laterally. A tubercle can be seen where the inferior surface of the clavicle is broken, which would be in the area of *M. subclavius* attachment. If this is the antimere to M.54053, it would indicate some asymmetry in muscularity if not robusticity.

M.54055 (GC 87 116) (Fig. 3)
Right
This specimen preserves only the diaphysis of a right clavicle. The bone is preserved medially to the sternal metaphysis just medial of the costoclavicular ligament attachment area, and laterally to the area of the trapezoid line. The bone is fairly slender and gracile, with a moderate curvature to the medial and lateral portions of the shaft. In section, the proximal portion of the shaft is a triangle with height larger than base, more distally the shaft is rectangular with length approaching twice the width. Cutmarks (possibly recent) can be seen on the inferior surface just proximal of the conoid tubercle and on the anterosuperior shaft at the lateral end of the *M. pectoralis major* attachment area.

The anterior surface of the shaft is mildly rugose, but becomes increasingly so laterally past the point of maximum proximal curvature up to the medial end of the *M. deltoideus* origin area. Around mid-shaft the anterior surface is flat and is delimited by a clear crest superiorly, likely demarcating the lateral part of the *M. pectoralis major* origin area, which is separated from the small *M. deltoideus* attachment area by a smooth gap of ca. 10mm. The scar for the deltoid muscle is a small patch of moderately rugose bone on the superior surface of the shaft, with a very thin and small shelf of bone projecting anteriorly. The *M. trapezius* insertion area is smooth.

On the inferior surface, there is an inferiorly projecting tubercle on the proximal end of the bone in the area of the attachment of *M. sternohyoid*. The costoclavicular ligament attachment area is an irregular oval bounded by a crest anteriorly (perhaps for *M. pectoralis*

Fig. 3 Right clavicle, M.54055, natural size. **3A**, superior; **3B** inferior.

major) that gives the attachment area a concave appearance. This crest continues laterally as a blunt ridge, mildly rugose at first but becoming smoother laterally, that continues the length of the proximal shaft. This ridge forms a small sulcus dorsally near the lateral end of the proximal shaft, in the region of the lateral end of the *M. subclavius* attachment. The conoid ligament is well defined, positioned on the very dorsal edge of the inferior surface and projecting directly inferiorly. The trapezoid line appears as an abnormally large tubercle (at least 10.5mm wide by more than 12mm long and projecting 2mm from the inferior surface of the acromial process). In anterior view this tubercle looks like a facet for a pseudoarthrosis with the coracoid, but when viewed from below there is indication of neither an articular surface nor polished bone. This tubercle appears to represent an 'enthesopathic' outgrowth (musculoskeletal stress marker: Hawkey & Merbs, 1995) of bone due to activity or, less likely, a pathological ossification of the trapezoid ligament.

Morphology

The Creswellian-associated claviculae from Gough's Cave represent a minimum of two individuals, a larger, relatively robust individual represented by the left and right claviculae M.54053 and M.54054 and a smaller, somewhat more gracile individual represented by the right clavicle M.54055. The complete left clavicle M.54053 is long and large relative to late Upper Palaeolithic male claviculae, and the right side M.54054 has mid-proximal shaft dimensions that are larger than or approximately equal to the mean values for the male

Table 1 Clavicular dimensions (mm).

Measurement	M.54053	M.54054	M.54055
Maximum length (M-1)	152	–	–
Articular length[a]	146.2	–	–
Conoid length[b]	115.9	–	[98]
Midshaft maximum diameter[c]	13.6	–	11.9
Midshaft minimum diameter[c]	11.0	–	9.1
Midshaft circumference (M-6)	39	–	33
Mid-proximal superoinferior diameter[d]	12.0	14.7	10.6
Mid-proximal anteroposterior diameter[d]	13.0	11.8	8.8
Mid-proximal circumference[d]	42	43	32
Proximal epiphyseal superoinferior diameter[e]	(22)	–	–
Proximal epiphyseal anteroposterior diameter[e]	15.9	–	–
Costal impression mediolateral diameter[f]	17.9	(23.1)	13.8
Costal impression dorsoventral diameter[f]	10.9	10.5	7.3
Conoid superoinferior diameter[g]	14.6	–	12.1
Conoid anteroposterior diameter[g]	17.8	–	13.5
Acromial superoinferior diameter[h]	10.9	–	–
Acromial anteroposterior diameter[h]	19.3	–	–

Martin numbers (M-#: Martin, 1928) for measurements are provided where appropriate.
[a] direct distance between the mid-points of the proximal and distal epiphyses.
[b] direct distance from the mid-point of the proximal epiphysis to the middle of the conoid tubercle.
[c] midshaft determined relative to articular length (midshaft position estimated for M.54055).
[d] taken at mid-conoid length (mid-proximal position estimated for M.54054 and M.54055).
[e] maximum (SI) and minimum (AP) diameters of the proximal epiphysis.
[f] mediolateral and dorsoventral diameters of the costoclavicular ligament attachment area.
[g] taken at the conoid tubercle perpendicular (SI) and parallel (AP) to the superior surface of the bone.
[h] acromial diameters taken perpendicular (SI) and parallel (AP) to the superior surface of the bone.

Table 2 Comparative clavicular osteometrics (mean, SD, n).

Right claviculae	M.54054	M.54055	U.P. ♂	U.P. ♀
Conoid length	–	[98]	111.3, 7.9, 8	103.6, 7.6, 4
Mid-proximal SI diameter	14.7	10.6	11.9, 1.9, 8	9.8, 0.6, 5
Mid-proximal AP diameter	11.8	8.8	11.7, 1.0, 8	10.2, 1.0, 5
Conoid SI diameter	–	12.1	11.7, 2.2, 8	10.4, 1.2, 6
Conoid AP diameter	–	13.5	17.5, 2.0, 8	15.4, 2.1, 6
Left claviculae	M.54053		U.P. ♂	U.P. ♀
Maximum length	152		145, 8.9, 8	128, –, 2
Articular length	146.2		141.8, 8.7, 8	125.6, –, 2
Conoid length	115.9		112.2, 9.5, 9	100.1, 5.8, 3
Mid-proximal SI diameter	12.0		11.0, 1.6, 12	9.7, 0.5, 5
Mid-proximal AP diameter	13.0		11.7, 0.8, 12	10.1, 1.2, 5
Conoid SI diameter	14.6		11.3, 2.0, 11	10.7, 0.4, 5
Conoid AP diameter	17.8		15.9, 2.0, 11	13.8, 1.3, 5

All measurements are in millimeters and are defined in Table 1.

comparative sample (Table 2). Both claviculae exhibit moderate to heavy rugosity of muscle scars and ligament attachment areas. M.54053 has greater mid-shaft cross-sectional strength measures than the left claviculae of the male specimens Gough's Cave 1 and Rocheriel 1 (Table 3). The right clavicle M.54054 is larger in some cross-sectional strength values than Gough's Cave 1 and smaller in others, likely reflecting shape differences related to differences in mechanical loading (and hence behavioral) histories of the collar bone in these two individuals. On the basis of size, robusticity and muscular rugosity, it seems reasonable to conclude that M.54053 and M.54054 derived from male individuals, and that they likely belonged to the same individual (see above). If they are indeed antimeres, the greater development of the *M. pectoralis major* origin scar and costoclavicular ligament scars on the right side would suggest a considerable degree of bilateral asymmetry in limb use and a right hand-dominant individual. Based on the different stages of sternal epiphyseal fusion in

the two sides, and again assuming both claviculae derive from the same person, this individual was probably between the ages of 18 and 25 at the time of death (Williams & Warwick, 1980).

The right clavicle M.54055 is much more gracile, in both external and cross-sectional dimensions (Tables 2 and 3). In overall size and shape this specimen compares most favourably with females of the comparative sample and thus probably represents a female, although the possibility that the specimen represents a juvenile male cannot be ruled out. Although the bone is relatively lightly constructed, the muscle scars (especially that of *M. deltoideus*) are fairly well defined and the costoclavicular ligament attachment area is rugose. The existence of a (possible) musculoskeletal stress marker at the attachment of the trapezoid ligament suggests that this individual engaged in a repetitive motion involving humeral abduction, since this motion engenders scapular rotation and stresses the acromioclavicular ligaments.

Table 3 Mid-shaft clavicular cross-sectional properties.

Right claviculae	M.54054	M.54055	GC1[a]
Total area (TA) (mm^2)	135.0	76.5	124.9
Cortical area (CA) (mm^2)	83.6	56.5	87.3
Medullary area (MA) (mm^2)	51.4	20.0	37.6
SI second moment of area (I_x) (mm^4)	1502.3	497.7	1319.8
DV second moment of area (I_y) (mm^4)	1026.3	387.2	1154.2
Maximum 2nd moment of area (I_{max}) (mm^4)	1502.5	540.6	1752.1
Minimum 2nd moment of area (I_{min}) (mm^4)	1026.2	344.3	721.9
Polar moment of area (J) (mm^4)	2528.7	884.9	2474.0
Percent cortical area (%CA)	61.9	73.9	69.9
I_x/I_y	1.46	1.28	1.14
I_{max}/I_{min}	1.46	1.57	2.43
Left claviculae	M.54053	GC1[a]	Roch1[b]
Total area (TA) (mm^2)	126.4	118.9	98.6
Cortical area (CA) (mm^2)	94.6	73.9	69.8
Medullary area (MA) (mm^2)	31.8	45.0	28.8
SI second moment of area (I_x) (mm^4)	1014.3	999.6	654.4
DV second moment of area (I_y) (mm^4)	1395.8	1084.4	784.1
Maximum 2nd moment of area (I_{max}) (mm^4)	1408.8	1505.1	824.6
Minimum 2nd moment of area (I_{min}) (mm^4)	1001.3	578.9	613.9
Polar moment of area (J) (mm^4)	2410.1	2084.0	1438.5
Percent cortical area (%CA)	74.8	62.2	70.8
I_x/I_y	0.73	0.92	0.83
I_{max}/I_{min}	1.41	2.60	1.34

[a] Gough's Cave 1.
[b] Rocheriel 1.

SCAPULAR REMAINS

M.54056 (M23.1/2 (1959)) (Figs 4–6)
Right
This specimen preserves a portion of the body, spine, coracoid process, axillary border and glenoid fossa of a right scapula (Fig. 4). The fragment measures ca. 123mm superoinferiorly by ca. 76mm mediolaterally. The spine is missing the acromion and all of its upper (superodorsal) border from the 'waist' (the point of minimum thickness between the acromion and the flared attachment for *M. deltoideus*) medially. Laterally the root of the spine is not preserved, nor is any of the vertebral border of the body. The superior surface of the spine is recently altered (from removal of a bone sample for direct dating), and most of the supraspinous fossa (including the superior angle) is absent from the suprascapular notch medially. Only the root of the coracoid is preserved, but virtually all of the glenoid fossa is intact (there is some damage or erosion to the ventroinferior margin). The axillary border is complete down to the distal origin of *M. teres major*.

The scapula exhibits numerous cutmarks. There is a series of obliquely oriented marks on the dorsal surface of the body in the infraspinous fossa, a few around the inferior ventral surface of the root of the coracoid and around the area of the supraglenoid tubercle, numerous marks running transversely across the dorsal pillar of the axillary border, and a series of superoinferiorly oriented marks on the dorsal surface at the *M. teres major* origin.

The glenoid fossa is a very broad piriform shape (Fig. 5). The articular surface is oriented slightly cranially and dorsally. There is a small (incipient) central pit evident on the articular surface. The attachment for the glenoid labrum can be clearly seen along most of the articular margin, especially so along the dorsal edge. No degenerative changes are evident on the articular surface.

There is only a small, smooth projection representing the supraglenoid tubercle, with a broad, diffuse attachment area (for the coracohumeral ligament and for the long head of *M. biceps brachii* ventrally) extending for 10–15mm along the superior dorsal margin of the glenoid fossa. The infraglenoid tubercle begins as a broad triangle whose base is positioned along the dorsal-most part of the inferior margin of the fossa. The tubercle is well developed and rugose. The tubercle continues distally as a high, thin dorsal pillar that forms the lateral edge of the axillary border. There is also a distinct tubercle on the ventroinferior margin of the glenoid, perhaps indicating a separate muscle slip from *M. triceps brachii*.

The axillary border exhibits a ventral sulcus (sulcus ventroaxillaris or sulcus axillaris subscapularis: Gorjanovic-Kramberger, 1914; von Eickstedt, 1925). The dorsal pillar (axillary scapular buttress on the dorsal scapular body: Smith, 1976) forms the extreme lateral edge of the border (Fig. 6). The groove for the circumflex scapular artery is clear. The axillary crest (crista medioaxillaris: Vallois, 1932) is lost superiorly in the rugosity of the infraglenoid tubercle, but can be made out on the dorsal pillar just superior of the groove for the circumflex scapular artery, and can be seen running directly inferiorly along the dorsal edge of the border. The crest is positioned, in its entirety, along the ventral edge of the dorsal pillar. The ventral pillar (ventral axillary scapular buttress) is strongly developed but is medially positioned (superiorly it begins below the middle of the coracoid root, inferiorly it converges with the dorsal pillar at the level of the *M. teres major* origin), and there is a wide, moderately deep ventral sulcus between the pillars.

The *M. teres minor* imprint is distinct (both superior and inferior areas) and a slight crest delineates the attachment area medially. The *M. teres major* origin area is preserved as a flattened facet that looks as if it continued laterally as a projection from the axillary border (postmortem breakage in this region makes evaluation of the morphology difficult). Some rugosity is evident along the *M. deltoideus* attachment area of the preserved portion of the spine.

This scapula belonged to an adult. The subcoracoid and inferior glenoid fossa rim secondary centres of ossification are both fully fused and the growth lines obliterated (both centres appear around
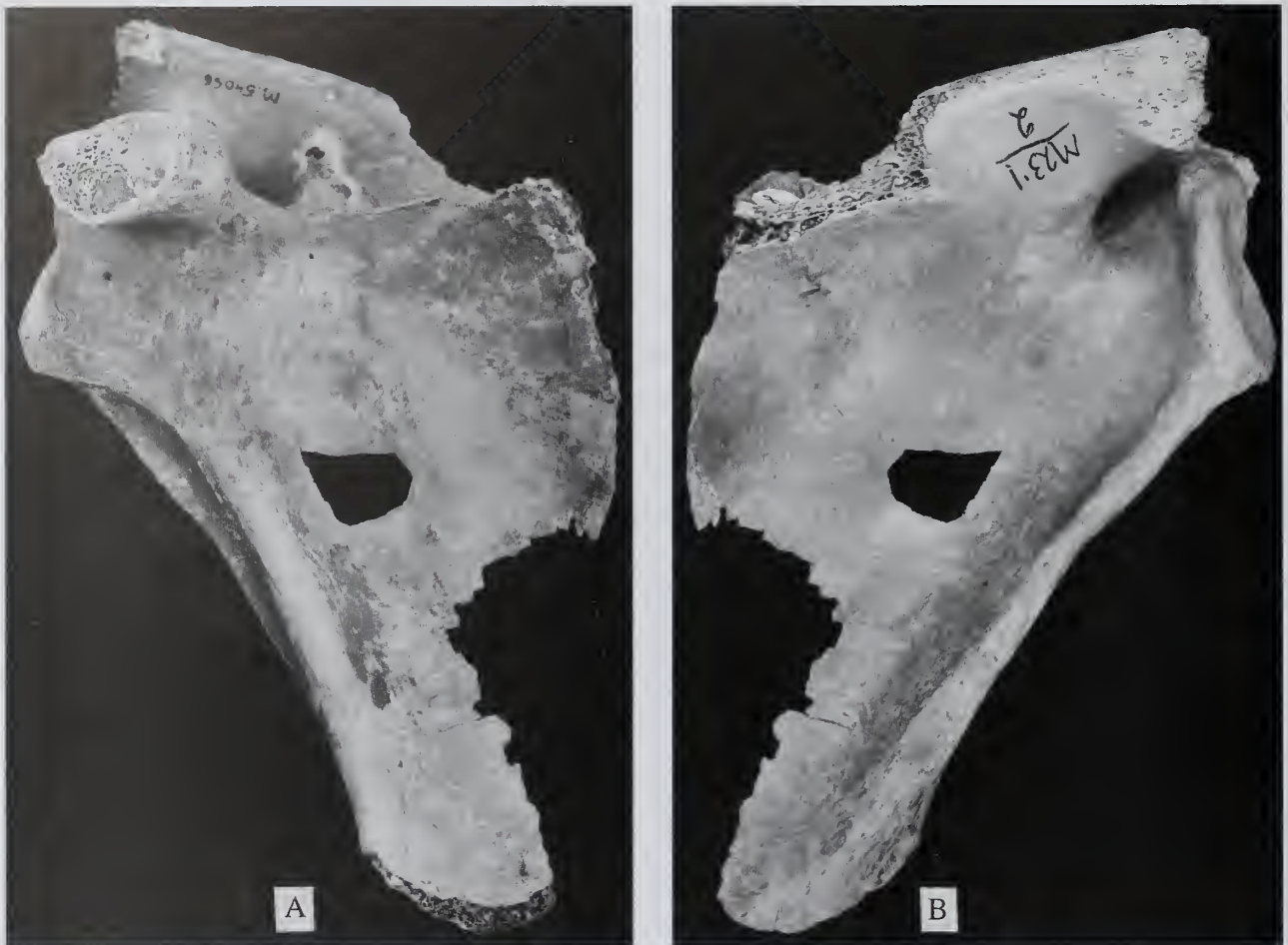
Fig. 4   Right scapula, M.54056, natural size. **4A,** ventral; **4B,** dorsal.

puberty and fuse by around age 20: Williams & Warwick, 1980). On the basis of size and morphology, this specimen is likely to have been the antimere of M.54057 (see below).

M.54057 (GC 87 266/89 012) (Figs 7, 8)
Left

Two fragments (GC 87 266 and 89 012) that join to form a portion of a left scapula, preserve the glenoid fossa, axillary border, body, and spine (Fig. 7). The total superoinferior length of the fragment is ca. 80mm and the mediolateral width is roughly 95mm. The spine continues medially to the vertebral border, but it is damaged along its superior margin, and the junction of the spine and vertebral border is not complete. The acromion is missing and the coracoid process is broken off at the root. The axillary border is complete and most of the body is present. Matrix adheres to parts of the body, spine and inferior axillary border. Scratches (perhaps cutmarks) are visible on the body, around the root of the spine, and on the dorsal aspect of the axillary border.

In size and morphology this specimen looks to be the antimere of M.54056. The glenoid fossa forms a broad piriform (Fig. 8), although not quite as dramatically as in the right scapula M.54056, and in other aspects of the morphology of the glenoid fossa and the supraglenoid tubercle, infraglenoid tubercle, axillary border and muscle markings this specimen is virtually identical to that of

M.54056 (with the single exception that there does not appear to be a second tubercle for the long head of *M. triceps brachii* on the inferoventral margin of the glenoid fossa).

As with M.54056, this scapula clearly belonged to an adult. The subcoracoid and inferior glenoid rim secondary centres of ossification

Table 4   Scapular dimensions (mm).

Measurement	M.54056	M.54057	M.54058
Morphological length (M-2)	–	(92.8)	–
Basal spinous length (M-8)	–	(75.2)	–
Mid-axillary border thickness[a]	(11.7)	–	9.8
Spino-glenoid angle (M-22)	88°	105°	(101°)
Axillo-glenoid angle (M-17)	48°	55°	38°
Axillo-spinal angle (M-16)	56°	50°	63°
Glenoid maximum length (M-12)	31.3	31.7	33.7
Glenoid maximum breadth (M-13)	26.9	25.4	(23.2)
Glenoid articular length[b]	28.0	29.5	30.8
Glenoid articular breadth[b]	25.2	24.3	23.1

Martin numbers (M-#: Martin, 1928) for measurements are provided where appropriate.

[a] dorsoventral diameter of the mid-axillary border, including dorsal and ventral pillars as present.

[b] Glenoid fossa length and breadth taken across the internal margins of the glenoid labrum attachment.

Fig. 5 Right scapula, M.54056, glenoid fossa in lateral view. 1.25x natural size.

are both fully fused and their growth lines are obliterated, indicating an age in the third decade or older (Williams & Warwick, 1980).

M.54058 (GC 1.1/38) (Fig. 9)
Left
This is a fragment of a left scapula, preserving most of the glenoid fossa (with damage only to the ventroinferior margin), the superior half of the axillary border, the lateral root of the spine, and the root of the coracoid process (Fig. 9). The fragment measures 89.6mm superoinferiorly and 57.0mm mediolaterally. Transversely oriented cutmarks can be seen on the axillary border.

The glenoid fossa is piriform in shape. The attachment of the glenoid labrum can be seen as a clear ridge along most of the margin of the articular surface. There is no evidence of degenerative changes to the joint surface, nor is there any indication of a central pit. The supraglenoid tubercle is small. There is a small, thin crest extending from the supraglenoid tubercle superiorly along the coracoid process, perhaps demarking the attachment area of the coracohumeral ligament. The infraglenoid tuberosity is large and long in the superoinferior direction (ca. 21mm) and comes off the inferodorsal aspect of the glenoid fossa rim. The infraglenoid tubercle is well developed and the entire surface of the tubercle is rugose. The axillary crest (crista medioaxillaris) runs directly inferiorly, maintaining its position along the dorsal part of the border until it reaches the broken edge of the border (ca. 55mm below the glenoid fossa

Fig. 6 Right scapula, M.54056, axillary border in lateral view. Natural size.

rim). The ventral pillar (ventral scapular axillary buttress) is well developed, broad and rounded, and forms a distinct, moderately deep ventral sulcus anterior of the axillary crest. The dorsal pillar (dorsal scapular axillary buttress) is thin and projecting, and is somewhat more laterally placed than the ventral pillar. The dorsal pillar is separated from the dorsal margin of the infraglenoid tubercle proximally by a clear sulcus (but the sulcus is evident only in the region of the infraglenoid tubercle). It then develops as a thin, high ridge that stops roughly 16mm inferiorly at the groove for the scapular circumflex artery. The intersection of the scapular circumflex artery and the axillary border is positioned relatively superiorly in this specimen. Below the groove the dorsal pillar is broader and forms the dorsal edge of the border.

The 'waist' of the superior border of the spine is preserved, as well as the superior surface another 37mm laterally. Fine matrix and sand adheres to the spine, nevertheless it is clear that the *Mm. deltoideus* and *trapezius* markings are not overly rugose. The scapular notch is very broad, the superior edge of the body forming an angle of about 110° with the medial edge of the coracoid process. The attachment
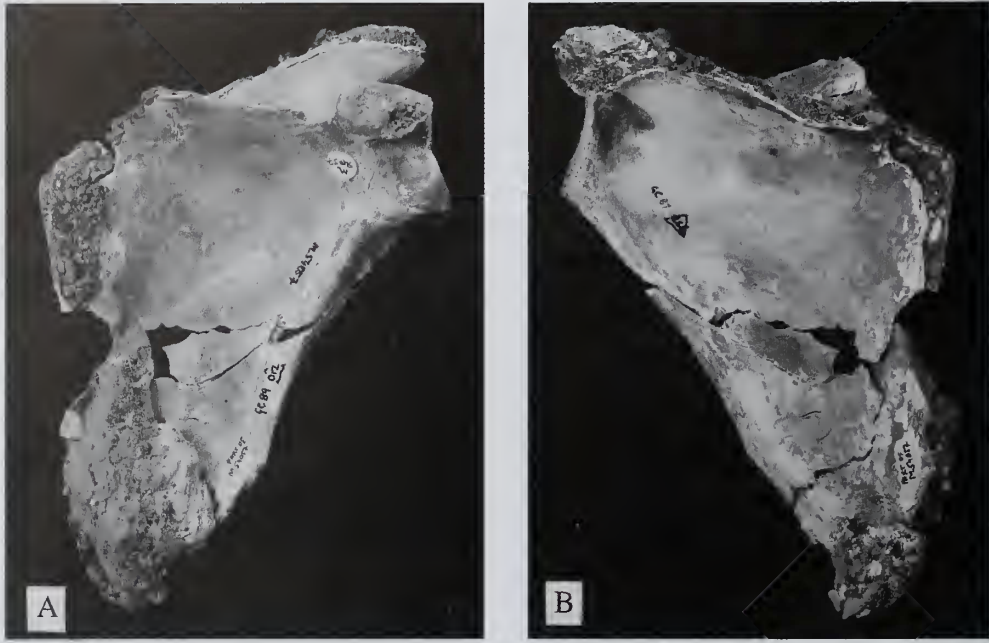
Fig. 7   Left scapula, M.54057, 0.5x natural size. **7A,** ventral; **7B** dorsal.

Fig. 8   Left scapula, M.54057, glenoid fossa in lateral view. Natural size.

area of the conoid ligament can be clearly seen as a smooth facet on the medial superior surface of the coracoid process.

The scapula was that of an adult. The subcoracoid and inferior glenoid fossa rim secondary centres of ossification are both fully fused and the growth lines are obliterated.

M.54059 (GC No. 7) (Fig. 10)
Left

This is a fragment of the lateral root and spine, plus portions of the body, of a left scapula (Fig. 10). The superior portion of the spine is missing and only the root is preserved. The total length of the fragment is 70.8mm superoinferiorly by 37.2mm dorsoventrally.

The scapular notch is preserved and forms a very open semicircle (with an angle of about 116° between the tangents to the two sides). The lateral edge of the notch is horizontal and the medial edge rises relatively steeply towards the superior angle. The notch is positioned close to the lateral root of the spine, and there is virtually no supraspinatus fossa in this specimen, at least on the lateral half of the scapula. The base of the glenoid is narrow ventrodorsally, and there is no indication of the superior end of the ventral pillar in the preserved portion. The subscapular surface abounds with scratch marks – perhaps of recent origin. Cutmarks are also visible on the lateral root of the spine.

Morphology

The scapular fragments from the Creswellian level of Gough's Cave represent a minimum of three individuals. The right and left scapulae M.54056 and M.54057 are morphologically very similar and are likely to derive from the same individual. Based on the overall size of these scapulae this individual was probably male, and judging from the degree of fusion of the observable secondary centres of ossification in the right-side scapula, he was over the age of twenty at the time of death. The left scapular fragment M.54058 also appears to have derived from a relatively large individual, and may likewise represent a male. Again judging from the degree of development of

Fig. 9 Left scapula, M.54058, 0.9x natural size. **9A**, ventral; **9B**, lateral; **9C**, dorsal.

secondary growth centres, this individual was also an adult. The left scapula M.54059 appears to have come from a smaller individual, perhaps either a female or a juvenile male.

All three of the preserved glenoid fossae have articular surfaces that are wide relative to their height (Table 5), especially those of M.54056 and M.54057. These two specimens have glenoid indices (100 × articular breadth/articular height) more than five (M.54056) and three (M.54057) standard deviations above the Upper Palaeolithic male mean index values. It is apparent from a comparison of their articular dimensions with those of other Upper Palaeolithic-associated fossils (Table 5) that these inflated index values are due to the relative superoinferior shortness of their glenoid articular surfaces.

Stringer (1985) saw the left scapula M.54058 as possessing a bisulcate axillary border, a feature that is fairly common in Upper Palaeolithic specimens. This specimen does exhibit, in addition to a ventrally positioned sulcus, a sulcus dorsal of the infraglenoid tubercle and proximal axillary crest. It is evident however that the dorsal sulcus does not extend distally more than a centimeter below the infraglenoid tubercle, and for this reason I think the specimen is
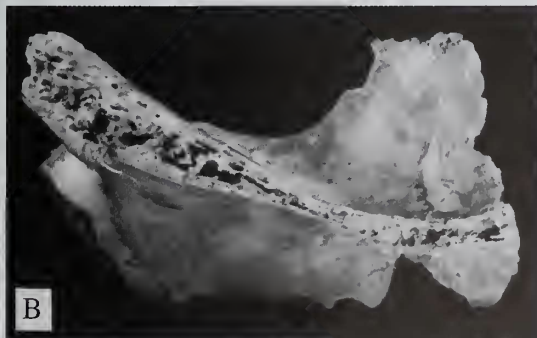

Fig. 10 Left scapula, M.54059, natural size. **10A**, ventral; **10B**, dorsal.

Table 5 Comparative scapular glenoid fossa articular dimensions.

	Articular length	Articular breadth	Glenoid Index[a]
M.54056 (right)	28.0	25.2	90.0
M.54057 (left)	29.5	24.3	82.4
M.54058 (left)	30.8	23.1	75.0
U.P. males			
right	36.1 ± 2.3 (6)	25.8 ± 2.2 (5)	72.3 ± 2.6 (5)
left	36.3 ± 1.2 (8)	25.6 ± 1.3 (7)	70.2 ± 3.5 (7)
U.P. females			
right	33.1 ± 1.1 (4)	23.7 ± 1.6 (4)	71.7 ± 5.5 (4)
left	33.2 ± 1.1 (4)	23.4 ± 0.8 (4)	70.5 ± 2.4 (4)

All measurements are in millimeters and are defined in Table 4.
[a] Glenoid index = (articular breadth/articular length) * 100.

Fig. 11   Gough's Cave humeral assemblage, anterior view, 0.5x natural size. From left to right: M.54062 (left humerus), M.54063 (left humerus), M.54060 (right humerus), M.54061 (right humerus).

perhaps better considered as possessing a ventral sulcus. The other preserved axillary borders exhibit well-developed ventral sulci as well. In a small sample of late Upper Palaeolithic specimens (n=17), Churchill (1994) found roughly equal proportions of ventral sulcate (53% of individuals) and bisulcate (47% of individuals) scapulae.

HUMERAL REMAINS

M.54060 (GC 1950–51, Level 12) (Fig. 11)
Right
This is a 96mm long fragment of a right humeral diaphysis, preserving only the ventrolateral surface (Fig. 11). The distal end of a relatively smooth deltoid tuberosity is preserved. In the vicinity of midshaft (at the distal end of the deltoid tuberosity) the lateral cortical thickness is 4.1mm.

M.54061 (GC 86 18/21) (Figs 11, 12)
Right
These are two diaphyseal fragments that conjoin to form a 180.9mm long portion of a right humeral shaft (Figs 11, 12). The preserved

Table 6   Dimensions (mm) of humeral fragment M.54061.

Midshaft maximum diameter (M-5)	(18.7) (midshaft location estimated)
Midshaft minimum diameter (M-6)	(15.4) (midshaft location estimated)
Midshaft circumference (M-7a)	[57] (midshaft location estimated)
Deltoid tuberosity width[a]	(6.9)

[a] distance between the apices of the delimiting crests of the tuberosity taken at 5/12's of humeral maximum length, following Endo (1971). In this case, the location of 5/12's maximum length was estimated.
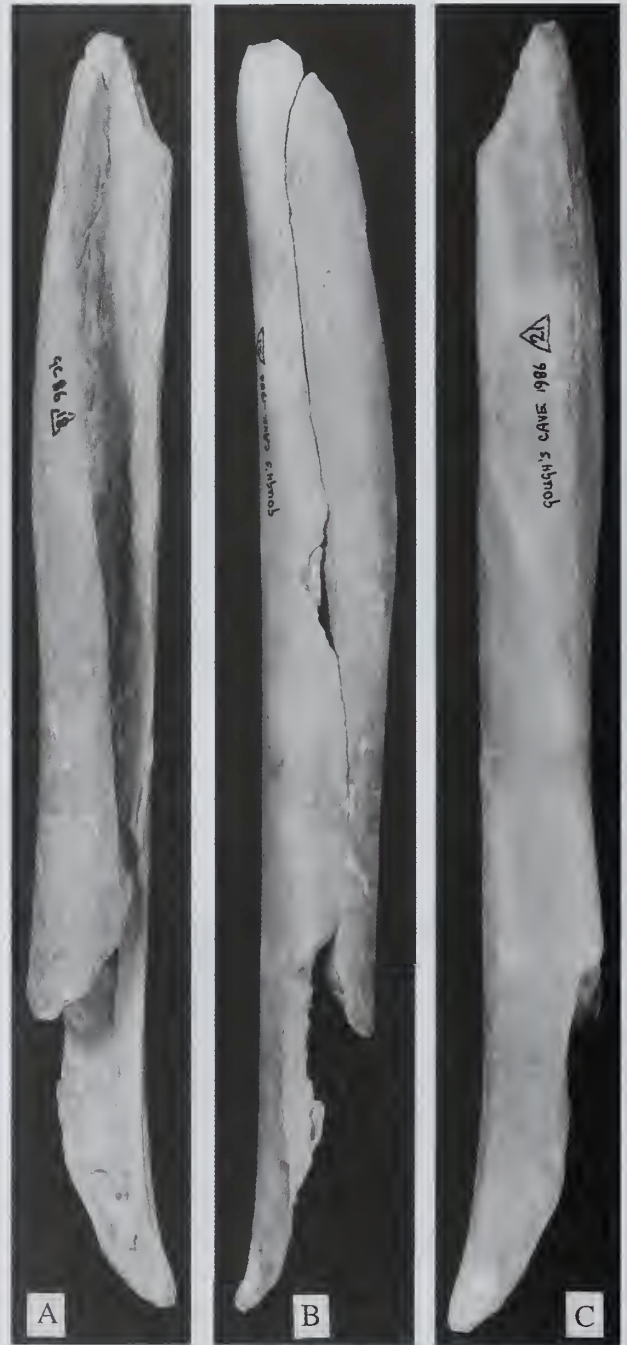

Fig. 12   Right humerus, M.54061, natural size. **12A**, anterior; **12B**, lateral; **12C**, posterior.

portion extends from just proximal of the proximal end of the lateral crest of the deltoid tuberosity to the distal shaft somewhere proximal of the olecranon fossa. The shaft is missing its medial surface for the entire length of the fragment, most of its anterior surface (preserving only the distal portion), and most of its anteromedial surface (preserving only the proximal portion).

The fragment is relatively small and gracile (Table 6), and the preserved muscle scar (*M. deltoideus*) is neither large nor rugose. Both crests of the deltoid tuberosity have faint muscle impressions.

The deltoid tuberosity appears to have been two-crested, with the crests being fairly close together.

M.54062 (GC 87 12/4) (Fig. 11)
Left

This is a 179.5mm long fragment of diaphysis of a left humerus. The bone is preserved from the anatomical neck proximally to the mid-distal shaft (in the vicinity of shaft minimum circumference) distally, with only the dorsomedial surface preserved. The bone is uniformly weathered and has a series of small marks (perhaps cutmarks) along the medial surface of the distal shaft.

The nutrient foramen is preserved on the distal medial surface. A part of the groove for the radial nerve is preserved, as is the proximal portion of the ridge for *M. coracobrachialis*. The *M. coracobrachialis* insertion is non-rugose. The dorso-lateral edge of the lateral ridge of *M. deltoideus* is visible along the lateral edge of the fragment. The preserved part of the deltoid tuberosity is non-rugose. The cortical bone is not markedly thick (at the mid-distal diaphysis, the medial cortical thickness measures 2.8mm and the dorsal thickness is 3.2mm). In overall size and morphology, this specimen could equally well have been the antimere of either M.54060 or M.54061.

M.54063 (GC Level 14) (Fig. 11)
Left

This is a 118.9mm long fragment of the diaphysis of a left humerus. The fragment preserves only the dorsomedial surface of the shaft from the region of the surgical neck (the proximal shaft begins to flare medially very mildly) proximally to the region around the nutrient foramen (and the proximal end of the *M. coracobrachialis* insertion) distally. This fragment preserves much of the same regions as the left humeral fragment M.54062 (see above), and therefore they obviously derive from two different individuals. Numerous cutmarks can be seen on the proximal medial surface, and a few cutmarks can also be seen overlying the *M. coracobrachialis* insertion scar.

A portion of the lateral ridge of the deltoid tuberosity is preserved in this specimen, and is only mildly rugose. The *M. coracobrachialis* scar is non-rugose. In the mid-distal shaft (in the vicinity of shaft minimum circumference) the medial cortex is 4.0mm thick, dorsally it is 4.6mm thick.

M.54064 (GC 87 153 A) (not figured)
This is a 28.8mm long by 25.4mm wide (maximum) triangular-shaped and mildly curved piece of diaphyseal bone. The cortical bone is thin (1.3mm at the edge) but the trabecular bone filling the internal (concave) surface is thick (9.1mm at its thickest point). It appears to represent a portion of the medial surface of the anatomical neck of a humerus.

M.54065 (GC 86 19) (not figured)
This specimen consists of two diaphyseal fragments of a larger long bone, possibly a humerus. The fragments are joined by matrix, and

matrix adheres to much of the external surface of one of the fragments. One of the fragments is tubular in shape and is 54.6mm long by 19.2 mm wide. The exposed external surface is slightly weathered, and one end of the internal surface shows some slight trabeculation (the other end is filled with matrix). The cortical bone at one edge is 3.1mm thick.

The second fragment is 75.0mm long by 14.2mm at its widest. It is not certain that this second fragment derives from the same bone as the first, and it is even questionable as to whether it is human.

Morphology

The humeral remains from this assemblage represent a minimum of three individuals. Two relatively small people are represented by the right-side humeral fragments M.54060 and M.54061. Both of these specimens preserve the distal portion of the deltoid tuberosity, and in both the muscle scar is non-rugose. The left-side fragment M.54062 also appears to derive from a smaller individual and also has a non-rugose deltoid tuberosity. This latter specimen could reasonably be associated with either of the right-side fragments. The left humeral fragment M.54063 clearly derives from a larger individual, one with mild rugosity of the deltoid tuberosity, and is unlikely to be the antimere of either of the right-side fragments, thus denoting a third individual.

Little can be said about the morphology of the Creswellian-associated humeri from Gough's Cave. In midshaft cross-sectional properties, the right-side M.54061 is well below even the Upper Palaeolithic female sample means in strength measures (Table 7), suggesting that this element may have belonged to a female or juvenile male. This single specimen also has, judging from the I_x/I_y ratio, a midshaft cross-section that was more resistant to bending in the anteroposterior plane than bending in the mediolateral plane, compared to humeri in the reference sample that are more nearly equal in resistance to bending moments in both planes (Table 7).

ULNAR REMAINS

M.54066 (GC 87 202, 243, 119c) (Figs 13, 14)
Right

This specimen is composed of six fragments that make up most of a right ulna (Fig. 13). Based on size and morphology, this specimen may be the antimere of M.54067 (see below). The total length of the rejoined fragment is ca. 220mm. Preservation of the two pieces making up the proximal end is very good (there is no erosion or weathering, only peri-/post-mortem breakage damage), whereas the fragments comprising the shaft are more heavily weathered. The proximal end is complete (save for the inferior half of the radial notch and the subjacent diaphysis) distally to the base of the coronoid

Table 7 Comparative humeral midshaft cross-sectional geometric properties (mean, SD, n).

	M.54061	U.P.♂	U.P.♀	Total U.P.
Total area (TA) (mm²)	220.0	334.5, 35.2, 10	271.0, 23.7, 6	309.3, 41.7, 18
Cortical area (CA) (mm²)	170.6	242.8, 44.5, 10	191.1, 44.8, 6	224.5, 47.7, 18
Medullary area (MA) (mm²)	49.4	91.7, 26.0, 10	79.8, 21.6, 6	84.7, 24.4, 18
AP 2nd moment of area (I_x) (mm⁴)	4626.1	8310.6, 1960.1, 10	5845.3, 1327.6, 6	7324.2, 1991.3, 18
ML 2nd moment of area (I_y) (mm⁴)	2978.5	8917.5, 2281.0, 10	5314.1, 1575.6, 6	7478.2, 2536.0, 18
Max. 2nd moment of area (I_{max}) (mm⁴)	4638.8	9246.5, 2353.5, 6	7432.4, 3166.8, 3	8476.8, 2511.9, 10
Min. 2nd moment of area (I_{min}) (mm⁴)	2965.7	5762.0, 941.9, 6	4211.7, 1262.3, 3	5286.1, 1182.3, 10
Polar 2nd moment of area (J) (mm⁴)	7604.5	17228.2, 4156.4, 10	11159.4, 2807.0, 6	14802.5, 4459.3, 18
Percent cortical area (%CA)	77.5	72.2, 8.5, 10	69.9, 9.5, 6	72.1, 8.6, 18
I_x/I_y	1.55	0.94, 0.09, 10	1.12, 0.17, 6	1.01, 0.14, 18
I_{max}/I_{min}	1.56	1.59, 0.27, 6	1.75, 0.46, 3	1.61, 0.33, 10

Fig. 13 Right ulna, M.54066, 0.5x natural size. 13A, anterior; 13B, lateral; 13C, posterior.

process on the volar surface. The dorsal and medial surfaces are complete distally to well past midshaft. Only portions of the volar surface of the shaft are preserved. The lateral surface of the shaft is the best preserved, and is almost completely represented from the

proximal end down to the level of the *M. pronator quadratus* crest distally.

The trochlear notch opens anteroproximally (the coronoid process is much higher than the olecranon) (Table 8 and Fig. 14). There is a distinct ridge separating the coronoid and olecranon articular surfaces in the trochlear notch, and there appears to be a small outgrowth of bone just distal of this ridge (on the coronoid articular surface) near the centre of the trochlear notch. There is no indication of degenerative changes to any of the proximal articular surfaces (including the preserved portion of the radial notch).

The proximal surface of the olecranon process is not very rugose, but vertical striations can be seen on the dorsal margin along the *M. triceps brachii* insertion. The area of the *M. anconeus* insertion is weathered and broken, but what is preserved of the muscle scar is non-rugose. The morphology of the proximal *M. supinator* crest cannot be evaluated because of damage to the medial shaft below the radial notch, but this muscle often extends distally well below the level of the *M. brachialis* scar and may overlap the proximal end of the interosseus crest. In the case of M.54066, the distal portion of the muscle attachment can be seen on the proximal shaft, where it is slight but clear, indicating a moderate-to-strong development of the supinator muscle. Only the distal half of the *M. brachialis* scar is preserved, which appears as a well defined, raised scar with clear borders. There is a thin yet clear crest for *M. pronator teres*, but no clear origin area for the ulnar head of *M. flexor digitorum superficialis* can be seen.

More distally, the interosseus crest is a clear, sharp line that diminishes around midshaft and then picks up again on the distal-most part of the fragment as a broader, rugose line. There is a pronounced medial deviation of the shaft at the level of the *M. brachialis* scar, but this may be a function of post-mortem damage and reconstruction of the shaft from numerous fragments. The cortical bone thickness in the proximal shaft (at the level of the beginning of the interosseus crest) is 2.0mm, while in the distal shaft (at the level of the *M. pronator quadratus* crest) it is 2.3mm thick.

M.54067 (GC 87 226 A) (Fig. 15)
Left
This is a proximal left ulna, with a total length of 58.1mm. This may represent the antimere of the right side ulna M.54066 (see above), and may come from the same bone as M.54068 (see below). Only the

Table 8 Ulnar dimensions (mm).

	M.54066	M.54067	M.54069
Olecranon length (M-8)	20.8	18.2	–
Olecranon height (M-7)	24.4	(25)	–
Olecranon breadth (M-6)	26.3	25.2	
Trochlear notch chord (M-7(1))	23.7	–	
Coronoid height[a]	37.1	–	–
Radial facet maximum diameter[b]	(>15)	–	–
Radial facet minimum diameter[b]	[9.5]	–	–
Diaphyseal sagittal trochlear angle (M-15a)	15°	–	
Proximal anteroposterior diameter[c]	18.1	–	14.7
Proximal transverse diameter[c]	18.9	–	11.3
Proximal circumference[c]	–	–	45
Crest anteroposterior diameter (M-11)	18.9	18.1	–
Crest mediolateral diameter (M-12)	21.6	21.9	–
Midshaft anteroposterior diameter[d]	(17.4)	–	–
Midshaft mediolateral diameter[d]	(17.5)	–	–
Midshaft circumference[d]	(53)	–	–

[a] maximum anteroposterior diameter from the dorsal surface of the bone to the anterior tip of the coronoid process (McHenry *et al.*, 1976).
[b] maximum and minimum diameters of the articular facet for the radial head.
[c] taken at the level of the distal border of the ulnar tuberosity (McHenry *et al.*, 1976).
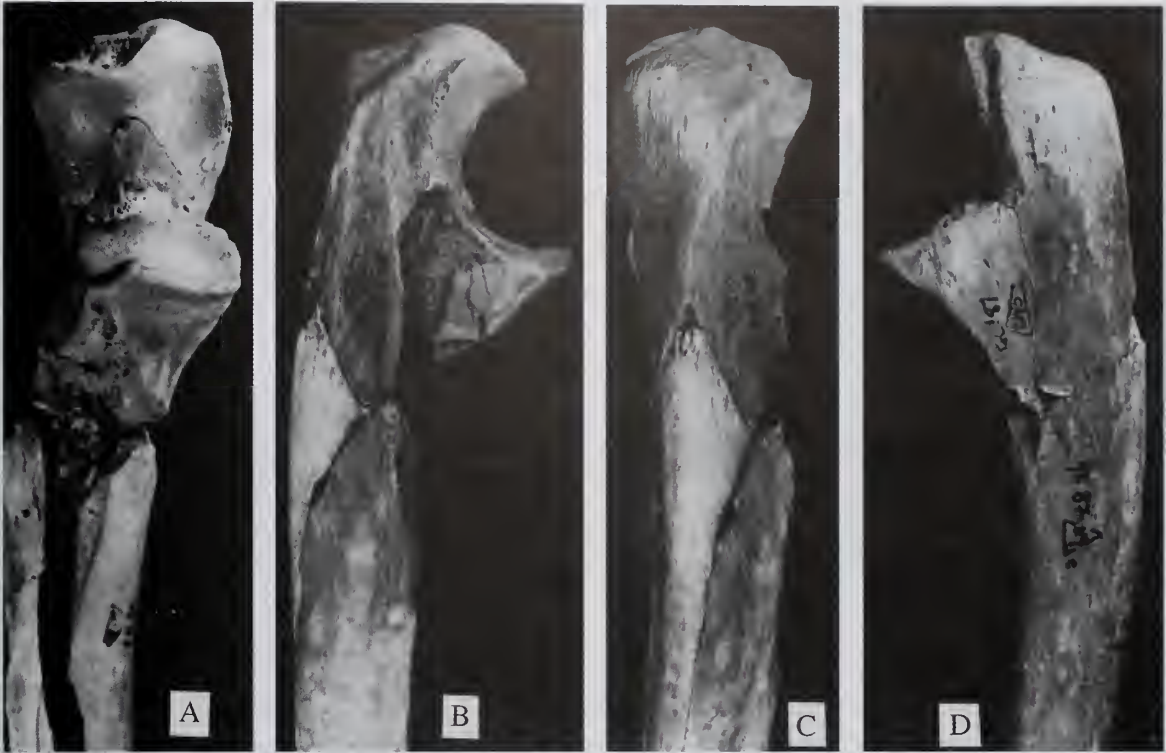[d] midshaft location estimated.

Fig. 14 Right ulna, M.54066, proximal, natural size. **14A,** anterior; **14B,** lateral; **14C,** posterior; **14D,** medial.
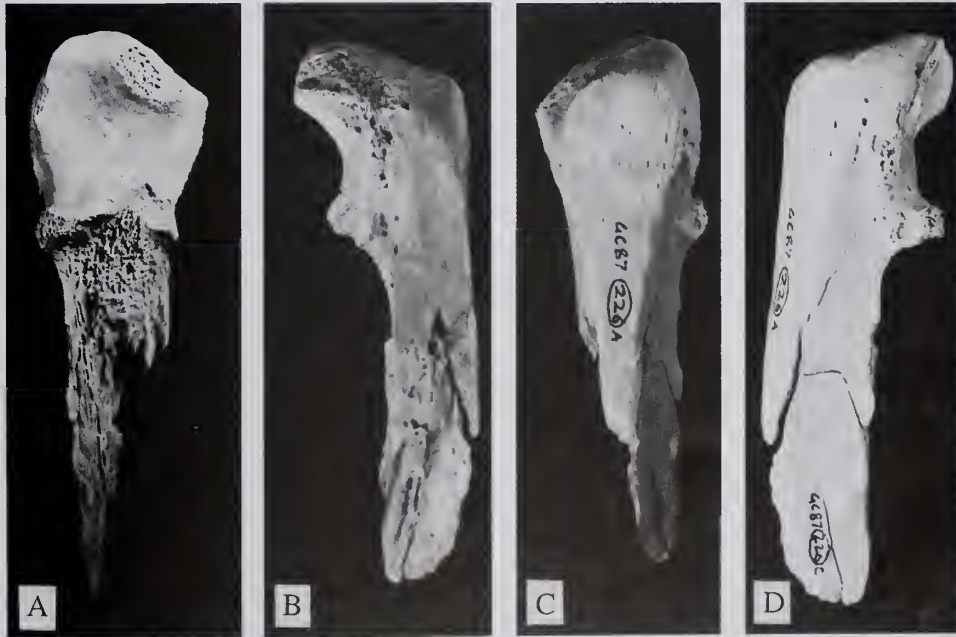

Fig. 15 Left proximal ulna, M.54067, natural size. **15A,** anterior; **15B,** lateral; **15C,** posterior; **15D,** medial.

olecranon process is preserved on the volar surface, and the entire coronoid process and volar surface of the shaft is missing distally. More bone is preserved on the dorsal surface, which is broken distally about half way along the *M. anconeus* insertion. There is some erosion to the volar-most tip of the olecranon process.

The *M. anconeus* insertion area is smooth, and the *M. triceps brachii* insertion is also non-rugose. A small portion of the proximal end of the *M. supinator* crest can be seen near the broken volar
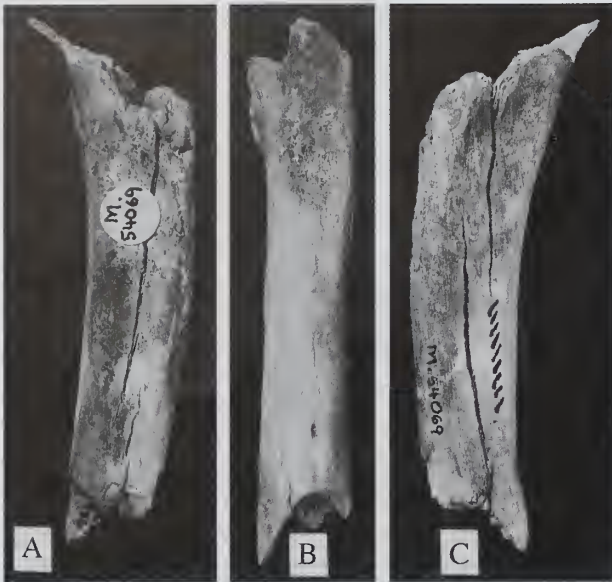
Fig. 16 Right ulna, M.54069, natural size. **16A,** medial; **16B,** anterior;
16C, lateral.

surface, and this crest is only mildly rugose. There is only a slight
crest evident separating the olecranon and coronoid articular sur-
faces in the trochlear notch.

M.54068 (GC 87 209) (not figured)
Left

This is a 121.2mm long (by 15.0mm wide) fragment of left ulnar
diaphysis. The fragment preserves only the dorsal surface (and part
of the dorsolateral surface up to the inferior edge of the interosseous
crest). The specimen is preserved from the region of the distal *M.
anconeus* insertion (with cutmarks at the very distal end of the
insertion area) proximally to around midshaft distally. Cutmarks can
also be seen on the dorsal surface at the very distal end of the
fragment.

The morphology of this specimen compares favourably with the
right ulna M.54066 (see above), and M.54068 may represent its
antimere and the distal portion of the left proximal ulnar fragment
M.54067 (see above).

M.54069 (GC 420.1: Level 12, 1950–51 excavations) (Fig. 16)
Right

This is a fragment of a right ulnar diaphysis, from just proximal of the
M. brachialis scar to just distal of the proximal end of the interos-
seous crest. The total length of the fragment is 70mm. The bone is
small and gracile and possibly represents a subadult. The bone
surface is weathered or calcined. Cutmarks are visible on the
superomedial margin of the diaphysis near the distal break.

The *M. brachialis* scar is not rugose but the muscle attachment
area can be clearly discerned. What appears to be the distal part of a
small *M. supinator* crest is visible on the lateral side. The *M.
anconeus* also appears to be only mildly rugose, but there is damage
to the inferior-proximal surface making evaluation of the muscle
marking morphology difficult.

M.54070 (GC 87 118 B) (not figured)
Left

This is a 47.8mm by 9.1mm diaphyseal fragment of the anteromedial
shaft of a distal left ulna. The fragment preserves the distal-most two
centimeters of the *M. pronator quadratus* crest (which is distinct but
not markedly large) and the metaphyseal region just proximal of the
head.

Morphology

The Gough's Cave Creswellian ulnar assemblage represents a mini-
mum of two individuals, one relatively large (male?) and one smaller
and more gracile (perhaps female or juvenile). The right ulnar
fragment M.54066 and the left ulnar fragments M.54067 and
M.54068 are sufficiently similar in size and morphology to suggest
that they derive from the same individual. Especially noteworthy is
the observation that both bones have generally non-rugose muscle
scars, yet both show a more pronounced (although still moderate)
development of the attachment area of *M. supinator*. While none of
these three specimens exhibit marked muscular rugosity, the external
dimensions of the bones tend to be comparable to or greater than the
mean values obtained for the late Upper Palaeolithic male sample
(Table 9), supporting the suggestion that these remains derive from
a male. In terms of mid-proximal shaft cross-sectional strength
measures (Table 10), the right ulna M.54066 falls above the values
obtained for the male specimen Gough's Cave 1.

A smaller individual is represented by the right ulnar fragment
M.54069. This specimen has proximal shaft dimensions that are
small even relative to Upper Palaeolithic females (Table 9).

Table 9 Comparative ulnar osteometrics (mean, SD, n).

Right ulnae	M.54066	M.54069	U.P.♂	U.P.♀
Olecranon length	20.8	–	16.8, 3.0, 11	16.7, 2.0, 4
Olecranon height	24.4	–	26.7, 1.8, 11	23.8, 1.4, 4
Olecranon breadth	26.3	–	25.7, 1.4, 10	24.1, 0.7, 3
Trochlear notch chord	23.7	–	26.8, 4.0, 8	22.7, 2.7, 3
Coronoid height	37.1	–	37.3, 1.8, 8	33.0, 1.1, 5
Radial facet maximum diam.	(>15)	–	16.4, 1.9, 7	16.4, –, 2
Radial facet minimum diam.	[9.5]	–	11.4, 0.7, 7	11.2, –, 2
Proximal AP diameter	18.1	14.7	15.1, 1.5, 8	15.9, 2.5, 3
Proximal transverse diam.	18.9	11.3	15.8, 1.5, 8	14.4, 0.5, 3
Proximal circumference	–	45	49.6, 3.2, 8	46.3, 2.5, 3
Left ulna	M.54067		U.P.♂	U.P.♀
Olecranon length	18.2		16.9, 2.9, 11	15.9, 2.1, 3
Olecranon height	(25)		25.0, 1.8, 11	21.4, 1.1, 3
Olecranon breadth	25.2		24.7, 2.0, 10	23.6, –, 1

All measurements are in millimeters and are defined in Table 8.

Table 10 Comparative right ulnar mid-proximal cross sectional geometric properties.

	M.5406	Gough's Cave 1
Total area (TA) (mm^2)	208.7	143.0
Cortical area (CA) (mm^2)	176.0	131.3
Medullary area (MA) (mm^2)	32.7	11.7
AP 2nd moment of area (I_x) (mm^4)	3641.9	1632.5
ML 2nd moment of area (I_y) (mm^4)	3529.8	1920.1
Max. 2nd moment of area (I_{max}) (mm^4)	4048.3	2096.7
Min. 2nd moment of area (I_{min}) (mm^4)	3123.3	1455.9
Polar 2nd moment of area (J) (mm^4)	7171.7	3552.6
Percent cortical area (%CA)	84.3	91.8
I_x/I_y	1.03	0.85
I_{max}/I_{min}	1.30	1.44

Fig. 17 Right radius, M.54071, natural size. **17A**, medial; **17B**, anterior; **17C**, lateral (note engraving).

RADIAL REMAINS

M.54071 (GC 87 60 A, 65, 74, 100, & 108 G) (Figs 17, 18)
Right

Five fragments conjoin to make up a portion of the mid-to-distal diaphysis of a right radius (Fig. 17). The dorsolateral surface of the diaphysis is engraved with a series of carat-shaped marks (Fig. 18: see also Andrews & Fernandez-Jalvo, this series of papers). The total length of the fragment is 156.1mm. Only a portion of the distal dorsal shaft and the lateral shaft (from midshaft region to the distal metaphyseal region) are preserved. On the distal-most part of the dorsal surface, several small nutrient foramina can be seen, as well as the beginning of the crest for *M. brachioradialis*. The fragment is broken medially before the dorsal (Lister's) tubercle. Proximally, a portion of the *M. pronator teres* scar can be seen on the superolateral shaft.

If the *M. pronator teres* scar is used as a rough indicator of midshaft, this specimen can be aligned with the estimated midshaft of the M.54066 ulna. Observation of the specimens in this alignment reveals that the two bones may well have belonged to the same individual. Furthermore, the overall size and morphology of this specimen matches well that of the left radial fragment M.54074/M.54075 (below), and likely represents its antimere.

M.54072 (GC 87 142) (Fig. 19)
Left

This specimen preserves 26.2mm of the anterior portion of the head and neck and the proximal margin of the radial tuberosity of a left radius. The articular rim is eroded on the medioposterior side of the head and the bone is missing from just posterior of the central depression of the head.

The anterior rim of the articular surface of the head does not dip distally towards the radial tuberosity as it does in most radii, but the same morphology can occasionally be seen in recent human radii (personal observation). The subperiosteal bone of the neck slopes mildly anteriorly and blends with the articular rim, such that there is not a steep drop-off from the articular to the non-articular surface as seen in most radii, but again a similar morphology can occasionally be found in recent human radii (personal observation).

The head is moderately large (mediolateral diameter of the head = 23.4mm; proximodistal length of the proximal ulnar facet = 6.2mm) and the neck appears wide (neck mediolateral diameter = 15.9mm). The proximal margin of the radial tuberosity appears to be relatively proximally positioned (*i.e.* is not very far down the shaft), suggesting a short head-neck length in this individual. This specimen may represent the antimere of M.54073 (see below).

M.54073 (GC 87 235) (not figured)
Right?

This is a fragment of a proximal radius including a portion of the proximal (capitular) articular surface, the anterior articular rim (preserving the 'dip' in the anterior articular surface) and a sliver of the neck down to the beginning of the radial tuberosity. The total fragment length is 24.2mm. When seen in anterior view, the superior articular surface seems to rise slightly to the right, suggesting that this represents a right side radius.

In addition to a general congruence in size, two aspects of morphology are similar to that seen in M.54072 (above). First, the distance from the articular surface (on the anterior aspect) to the beginning of the *M. biceps brachii* scar is the same as that of M.54072. Second, the distal margin of the anterior articular surface slopes onto the neck subperiosteal surface, with no sharp drop. This specimen most likely represents the antimere of M.54072.
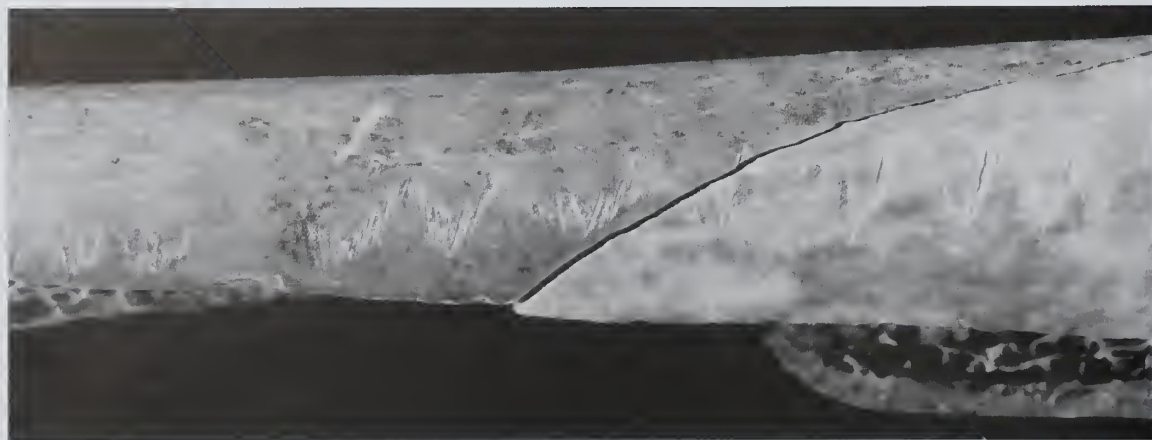
Fig. 18 Right radius, M.54071, detail of engravings. 3x natural size.
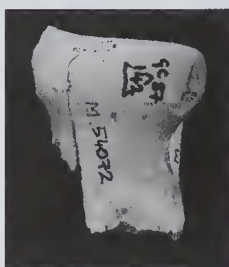

Fig. 19 Left proximal radius, M.54072, anterior view. Natural size.

M.54074, M.54075 (GC 87 65, 100, 108 E, 118 A, 123 C & 152) (Fig. 20)
Left
Six fragments conjoin to form a portion of the diaphysis of a left radius. The diaphysis preserves only a small portion of the volar surface along the medial side from just inferior of the radial tuberosity to distal of midshaft, as well as some volar surface in the distal metaphyseal region. Virtually the entire medial surface, preserving the interosseous crest, is present from just distal of the radial tuberosity to the distal metaphysis. Dorsally, only the medial side of the proximal shaft is preserved, but the dorsal surface is largely complete from the region of midshaft to the distal metaphysis. None of the distal articular surfaces are preserved, but the medial-most dorsal (Lister's) tubercle is preserved. The lateral surface of the shaft is present only in the region of midshaft, where it preserves a portion of the *M. pronator teres* insertion, which is well defined and rugose.

In size and morphology this specimen matches M.54071 (above), and probably represents its antimere.

M.54076 (GC 1949–51 Level 13) (not figured)
Right
This specimen preserves 110.3mm of a right radial diaphysis. The fragment preserves a portion of the interosseus crest and the distal end of the anterior ridge (the ridge that extends distally from the radial tuberosity and gives rise to the radial head of *M. flexor digitorum superficialis*). The proximal portion of the shaft preserves some of the lateral and dorsal surfaces, while distally only the medial and dorsal surfaces are preserved.

Morphology

Little can be said about the comparative morphology of the Gough's Cave radii, since muscle scars and articular surfaces are poorly represented. The five Creswellian radial remains described above may all derive from a single individual. This individual was probably male (on the basis of size and the moderate rugosity of the *M. pronator teres* scar in M.54074/M.54075), adult (judging from the state of fusion of the preserved portion of the distal epiphysis in M.54071) and may be the same individual represented by the fragmentary ulna M.54066.

MANUAL REMAINS

M.54077 (GC 87 221(?)) (not figured)
This specimen preserves the head of a metacarpal, probably from the fourth or fifth ray, side indeterminate. The distal epiphysis is fully fused.

M.54078 (GC 87 221 D) (not figured)
Right
This is a 56.0mm long fragment of the diaphysis of what is most likely a right second metacarpal. The specimen preserves a small bit of articular surface proximally that likely represents the third metacarpal articular facet, and an epiphyseal plate distally (with the head unfused). The metacarpal heads usually unite with the shafts in the

Table 11   Dimensions (mm) of manual phalanx fragment M.54079.

Midshaft height[a]	7.0
Midshaft breadth[a]	(11.8)
Midshaft circumference[a]	(33)
Distal height[b]	8.0
Distal maximum breadth[c]	11.7
Distal articular height[d]	11.2

[a] Maximum dorsovolar and radioulnar diameters and circumference at midshaft (midshaft location estimated). In the case of breadth and circumference, the proximodistal crack in the palmar surface of the bone has slightly inflated the measurements.
[b] Dorsovolar diameter of the head.
[c] Maximum radioulnar diameter of the head.
[d] Maximum radioulnar diameter of the articular facet of the head.

Fig. 20   Left radius, M.54074 and M.54075, natural size. **20A,** anterior; **20B,** medial; **20C,** posterior; **20D,** lateral.

fifteenth to sixteenth year in females, or in the eighteenth to nine-teenth year in males (Williams & Warwick, 1980).

M.54079 (GC 87 175 A) (Fig. 21)

This specimen is a proximal phalanx lacking its proximal end, with a total length of 37.7mm (Fig. 21). The side is indeterminate. The proximal end is damaged and the epiphysis is missing. The damage is close to the epiphyseal line (the nutrient foramina are visible) but not enough of the region survives to know whether or not the

epiphysis was fused. There is a large crack running proximodistally along the palmar surface of the diaphysis, as well as some damage to one side of the shaft at the proximal end. The transverse diameter of the shaft expands gradually from distal to proximal, and in this aspect the specimen most closely resembles that of a proximal phalanx from the third or fourth ray. The crests for attachment of the fibrous sheaths for *Mm. flexor digitorum profundus* and *f. d. superficialis* are well marked and prominent on this specimen.
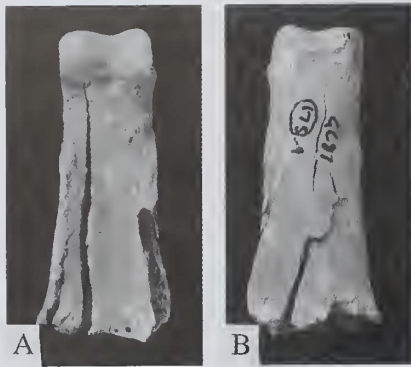
Fig. 21   Proximal phalanx, M.54079, natural size. **21A**, palmar; **21B**, dorsal.

REFERENCES

Bonin, G. von 1935. The Magdalenian Skeleton from Cap-Blanc in the Field Museum of Natural History. *University of Illinois Bulletin*, **34**: 1–76.

Boule, M. & Vallois, H. V. 1946. *Les Hommes Fossiles*. Paris.

Breuil, H. 1912. Les subdivisions du Paléolithique supérieur et leur signification. *Congres Internationale Anthropologie, Archéologie et Préhistoire*, Genève, **14**: 165–238.

Churchill, S. E. 1994. *Human Upper Body Evolution in the Eurasian Later Pleistocene*. Ph.D. thesis, University of New Mexico.

Cook, J. 1986. Marked human bones from Gough's Cave, Somerset. *Proceedings of the University of Bristol Spelaeological Society*. **17**: 275–285.

Currant, A. P., Jacobi, R. M. & Stringer, C. B. 1989. Excavations at Gough's Cave, Somerset 1986–7. *Antiquity*, **63**: 131–136.

Eickstedt, E.F. von 1925. Variationen am Axillarrand der Scapula (Sulcus axillaris teretis und Sulcus axillaris subscapularis). *Anthropologischer Anzeiger*, **2**: 217–218.

Endo, B. 1971. Some characteristics of the deltoid tuberosity of the humerus in the West

Asian and European 'classic' Neandertals. *Journal of the Anthropological Society of Nippon*, **79**: 249–258.

Eschman, P.N. 1990. *SLCOMM*. Albuquerque.

Genet-Varcin, E. & Miquel, M. 1967. Contribution à l'étude du squelette magdalénien de l'abri Lafaye à Bruniquel (Tarn et Garonne). *Anthropologie, Paris*, **71**: 467–478.

Gieseler, W. von 1977. Das jungpaläolithische Skelett von Neuessing. *In*: P. Schröter (ed). *75 Jahre Anthropologishe Staatssammlung München*: 39–51, München.

Gorjanovic-Kramberger, D. 1914. Kiefergelenk des diluvialen Menschen aus Krapina in Kroatien. *Vijesti geolosko povjerenstvo za godine, 1912–1914*: 182–184.

Hawkey, D. E. & Merbs, C. F. 1995. Activity-induced musculoskeletal stress markers (MSM) and subsistence strategy changes among ancient Hudson Bay Eskimos. *International Journal of Osteoarchaeology*, **5**: 324–338.

Martin, R. 1928. *Lehrbuch der Anthropologie, 2nd Edition*. Jena.

McHenry, H.M., Corruccini, R.S. & Huwell, F.C. 1976. Analysis of an early hominid ulna from the Omo Basin. *American Journal of Physical Anthropology*, **44**: 295–304.

Nagurka, M. L. & Hayes, W. C. 1980. An interactive graphics package for calculating cross-sectional properties of complex shapes. *Journal of Biomechanics*, **13**: 59–64.

Paoli, G., Parenti, R. & Sergi, S. 1980. *Gli Scheletri Mesolitici della Caverna delle Arene Candide (Liguria)*. Memorie dell'Istituto Italiano di Paleontologia Umana, No. 3. Rome.

Pittard, E. & Sauter, M. R. 1945. Un squelette magdalénien provenant de la station des Grenouilles (Veyrier, Haute-Savoie). *Archives suisses d'Anthropologie générale*, **11**: 149–200.

Sauter, M. R. 1957. Étude des vestiges osseux humains des grottes préhistoriques de Farincourt (Hte Marne, France). *Archives suisses d'Anthropologie générale*, **22**: 6.

Seligman, C. G. & Parsons, F. G. 1914. The Cheddar Man: a skeleton of late Palaeolithic date. *Journal of the Royal Anthropological Institute*, **44**: 241–263.

Smith, F. H. 1976. *The Neandertal Remains from Krapina: A Descriptive and Comparative Study*. University of Tennessee, Department of Anthropology Report of Investigation No. 15, Knoxville, TN.

Stasi, P. E. & Regalia, E. 1904. Grotta Romanelli (Castro, Terra d'Otranto). Stazione con faune interglaciali calda e di steppa. *Archivio per l'Antropologia e la Etnologia* **34**: 29–30, 39.

Stringer, C. B. 1985. The hominid remains from Gough's Cave. *Proceedings of the University of Bristol Spelaeological Society*, **17**: 145–152.

Vallois, H. V. 1932. L'omoplate humaine. *Bulletins et Mémoires, Société d'anthropologie de Paris*, **8**: 3–153.

—— 1941–1946. Nouvelles recherches sur le squelette de Chancelade. *Anthropologie*, Paris **50**: 65–202.

Verworn, M., Bonnet, R. & Steinmann, G. 1919. *Der diluviale Menschenfund von Oberkassel bei Bonn*: 6–10, Wiesbaden.

Williams, P. L. & Warwick, R. 1980. *Gray's Anatomy, 36th Edition*. Philadelphia.